Molecular Vision 2014; 20:307-324 <http://www.molvis.org/molvis/v20/307>
Received 19 November 2013 | Accepted 11 March 2014 | Published 14 March 2014

The erythropoietin receptor is not required for the development, function, and aging of rods and cells in the retinal periphery

Christian Caprara,[1] Corinne Britschgi,[1] Marijana Samardzija,[1] Christian Grimm[1,2,3]

[1]Lab for Retinal Cell Biology, Department of Ophthalmology, University of Zurich, Switzerland; [2]Zurich Center for Integrative Human Physiology, University of Zurich, Switzerland; [3]Neuroscience Center Zurich, University of Zurich and ETH Zurich, Switzerland

Purpose: Erythropoietin (EPO) was originally described for its antiapoptotic effects on erythroid progenitor cells in bone marrow. In recent years, however, EPO has also been shown to be cytoprotective in several tissues, including the retina. There, exogenous application of EPO was reported to exert neuro- and vasoprotection in several models of retinal injury. EPO and the erythropoietin receptor (EPOR) are expressed in the retina, but the role of endogenous EPO-EPOR signaling in this tissue remains elusive. Here, we investigated the consequences for cell physiology and survival when *EpoR* is ablated in rod photoreceptors or in the peripheral retina.

Methods: Two mouse lines were generated harboring a cyclization recombinase (CRE)-mediated knockdown of *EpoR* in rod photoreceptors (*EpoR*$^{flox/flox}$*;Opn-Cre*) or in a heterogeneous cell population of the retinal periphery (*EpoR*$^{flox/flox}$*;α-Cre*). The function of the retina was measured with electroretinography. Retinal morphology was analyzed in tissue sections. The vasculature of the retina was investigated on flatmount preparations, cryosections, and fluorescein angiography. Retinal nuclear layers were isolated by laser capture microdissection to test for *EpoR* expression. Gene expression analysis was performed with semiquantitative real-time PCR. To test if the absence of EPOR potentially increases retinal susceptibility to hypoxic stress, the knockdown mice were exposed to hypoxia.

Results: Newborn mice had lower retinal expression levels of *EpoR* and soluble *EpoR* (*sEpoR*) than the adult wild-type mice. In the adult mice, the *EpoR* transcripts were elevated in the inner retinal layers, while expression in the photoreceptors was low. CRE-mediated deletion in the *EpoR*$^{flox/flox}$*;Opn-Cre* mice led to a decrease in *EpoR* mRNA expression in the outer nuclear layer. A significant decrease in *EpoR* expression was measured in the retina of the *EpoR*$^{flox/flox}$*;α-Cre* mice, accompanied by a strong and significant decrease in *sEpoR* expression. Analysis of the retinal morphology in the two knockdown lines did not reveal any developmental defects or signs of accelerated degeneration in the senescent tissue. Similarly, retinal function was not altered under scotopic and photopic conditions. In addition, *EpoR* knockdown had no influence on cell viability under acute hypoxic conditions. Retinal angiogenesis and vasculature were normal in the absence of EPOR. However, expression of some EPOR-signaling target genes was significantly altered in the retinas of the *EpoR*$^{flox/flox}$*;α-Cre* mice.

Conclusions: Our data suggest that expression of EPOR in rod photoreceptors, Müller cells, and amacrine, horizontal, and ganglion cells of the peripheral retina is not required for the maturation, function, and survival of these cells in aging tissue. Based on the expression of the EPOR-signaling target genes, we postulate that expression of soluble EPOR in the retina may modulate endogenous EPO-EPOR signaling.

The cytokine erythropoietin (EPO) has long been recognized as the principal hormonal regulator of erythropoiesis, stimulating the growth and promoting the differentiation of early erythroid progenitor cells [1]. In the adult, this cytokine is produced mainly by the kidney, and is secreted into the blood circulation to reach the bone marrow [2]. There, EPO binds to the cognate EPO receptor (EPOR) on erythroid progenitor cells, thus preventing apoptosis and stimulating their differentiation and maturation into erythrocytes [3]. The expression of *Epo* is oxygen-regulated, and is induced by hypoxia-inducible factors when tissue oxygenation is reduced [4]. Therefore, EPO secretion increases under hypoxic conditions, eventually resulting in an increase in the hematocrit [5].

The source of *Epo* expression is not limited to the kidney. In fact, about 10% of EPO found in the bloodstream is of non-renal origin [6]. Numerous tissues, including the brain, have been identified as secreting EPO (reviewed in [7]). Similarly, *EpoR* expression is broader than originally reported, being present in, among others, the brain, heart, and liver [8]. Expression of *Epo* and *EpoR* has also been found in the retina [9,10]. The widespread tissue distribution of EPOR proposes that the antiapoptotic effects of EPO may go well beyond the prosurvival effects on early erythroid progenitors. In fact, the tissue-protective abilities of this cytokine have been demonstrated in various experimental injury models over the last few years. For example, exogenous application of

Correspondence to: C. Grimm, University of Zurich, Ophthalmology, Laboratory for Retinal Cell Biology, Wagistrasse 14, Schlieren, 8952, Switzerland; Phone: +41 44 556 3001; FAX: +41 44 556 3999; email: cgrimm@opht.uzh.ch

EPO protected kidney and heart cells against injury provoked by ischemia reperfusion [11-13], and was neuroprotective in different brain injury models [14]. Neuroprotective effects of EPO have also been reported in the retina, including protection of retinal ganglion cells (RGCs) in experimental degenerative models [15-18], as well as preservation of photoreceptor survival after light exposure [19]. Much research effort has been put into elucidating the ability of exogenous applications of EPO to prevent cell death in view of the potential use of this cytokine as a therapeutic agent against degenerative diseases. However, the function of endogenous EPO-EPOR signaling in extrahematopoietic tissues, including the retina, has not yet been fully clarified. This is in part due to the embryonic lethal phenotype of *Epo* null and *EpoR* null mice, which die in utero because of impaired production of mature red blood cells [20,21].

In the brain, EPOR is thought to be required for neural progenitor cell (NPC) proliferation and thus for correct brain development. In fact, lack of *EpoR* results in severe impairment in embryonic neurogenesis [22,23]. A similar mechanism might be present in the developing retina; that is, EPO-EPOR signaling may be essential for retinal progenitor cell (RPC) proliferation, in particular during the period of physiologic hypoxia in postnatal retinal development [24]. In addition to neuroprotection, EPO-EPOR signaling has been linked to developmental angiogenesis through angiogenic and vasoprotective properties [25]. Deletion of *Epo* or *EpoR* in mice severely affected angiogenesis and resulted in reduced complexity of the vessel networks, characterized by narrower vessel diameter and reduced vascular branching [26]. Consequently, the absence of EPO-EPOR signaling in the early postnatal mouse retina could potentially impair angiogenesis. To address these questions, we generated a conditional knockdown mouse line lacking the *EpoR* gene in a heterogeneous cell population of the retinal periphery. We show that the absence of EPOR did not result in overt defects in maturation, angiogenesis, and function of the peripheral retina in these mice, and that the tissue survived acute hypoxic exposure.

EPO-EPOR signaling may be implicated not only in retinal development but also in the ability of retinal cells to cope with chronic stress, which could impair long-term survival. In the adult retina, EPO and EPOR expression follows a circadian rhythm, with increased protein levels before the onset of daily light [27]. This expression pattern hints at a possible role of EPO-EPOR signaling in coping with increased phototoxic stress during the day. To test whether rod-specific *EpoR* expression is necessary for long-term photoreceptor survival, we generated a conditional knockdown mouse line with a rod-specific ablation of *EpoR*. We found that expression of EPOR is not necessary for the function and survival of rod photoreceptors.

METHODS

Animals and genotyping: All animal experiments were conducted according to the regulations of the Cantonal Veterinary Authority of Zurich and the statement of the Association for Research in Vision and Ophthalmology (ARVO) for the use of animals in ophthalmic and vision research. All mice were kept at the animal facility of the University Hospital Zurich in a 12 h:12 h light-dark cycle with food and water ad libitum. Light was maintained at 60 lux at cage level during the light period. Mice were euthanized by CO_2 inhalation followed by cervical dislocation. All experiments were conducted with a minimum of n = 3 mice for each time point and condition.

Conditional *EpoR* knockdowns were generated by breeding $EpoR^{flox/flox}$ mice [23] carrying *loxP* sites in exons 1 and 4 of *EpoR* either to mice expressing *Cre* recombinase under control of the α-element of the *Pax6* promoter (*α-Cre*) [28] resulting in $EpoR^{flox/flox}$;*α-Cre* double mutant animals or to mice expressing *Cre* recombinase under control of the rhodopsin promoter (*Opn-Cre*) [29] resulting in $EpoR^{flox/flox}$;*Opn-Cre* double mutant mice. $EpoR^{flox/flox}$ littermates were used as controls. All mice were on a mixed BL/6;129S6 background and homozygous for the $Rpe65^{450Leu}$ allele. C57BL/6 mice were used to analyze postnatal gene expression. To investigate the spatial expression pattern of *Cre* recombinase in the *α-Cre* retina, *α-Cre* mice were crossed to *Ai6* reporter mice (stock number: 007,906, Jackson Laboratory, Bar Harbor, ME) that express ZSGREEN upon CRE-mediated recombination of a floxed STOP cassette [30]. The retinas were cryosectioned and analyzed for native ZSGREEN expression with fluorescent microscopy. Spatial activity of CRE recombinase in the *Opn-Cre* mice has been previously reported [31]. The mice were genotyped using genomic DNA isolated from ear biopsies with conventional PCR using the following conditions: initial denaturation (95 °C, 5 min); 35 cycles of denaturation (95 °C, 45 s), annealing (temperature see Table 1, 45 s) and elongation (72 °C, 45 s); and final extension (72 °C, 10 min). Primer pairs and annealing conditions are shown in Table 1. PCR products were run on a 1.5% agarose gel for size detection.

RNA isolation, cDNA synthesis, and semiquantitative real-time PCR: Retinas were isolated through a corneal incision and immediately snap frozen in liquid nitrogen. Total RNA was isolated using the RNeasy isolation kit (RNeasy, catalogue number: 74,104; Qiagen, Hilden, Germany) or the High

Table 1. Primers used for genotyping.

Gene	Forward primer (5′-3′)	Reverse primer (5′-3′)	Annealing temperature (°C)
EpoR^{flox}	(Common) CTCCAGCCCAGTCCACCAACTGGG	(WT, LOXP) GGCGGGTAGTGGTACAGCACTTGCC (DEL) CCCGTTCTTGGCTCAAAGCCAATC	67
Cre	GGACATGTTCAGGGATCGCCAGGCG	GCATAACCAGTGAAACAGCATTGCTG	67
Ai6	(WT) AAGGGAGCTGCAGTGGAGTA (MUT) AACCAGAAGTGGCACCTGAC	(WT) CCGAAAATCTGTGGGAAGTC (MUT) GGCATTAAAGCAGCGTATCC	62

Primer sequences of forward/reverse primers are shown in 5′-3′ orientation, together with annealing temperatures and size of the obtained amplicon. Shown are forward and reverse primers (5′-3′ orientation) used for genotyping, together with annealing temperatures.

Pure RNA isolation kit (catalogue number: 11,828,665,001; Roche Diagnostics, Basel, Switzerland). Residual genomic DNA was removed by an incubation step with DNase. RNA (650 ng or 1000 ng) was reverse transcribed using oligo(dT) and M-MLV reverse transcriptase (catalogue number: M1701; Promega, Madison, WI). Ten nanograms of cDNA were used for gene expression analysis with semiquantitative real-time PCR using a LightCycler 480 instrument (Roche Diagnostics), the LightCycler 480 SYBR Green I Master kit (catalogue number: 04,887,352,001; Roche Diagnostics), and specific primer pairs (Table 2). The primer pairs were designed to span large intronic sequences or to cover exon-exon boundaries. Gene expression was normalized to *actin beta* (*Actb*), and relative quantification was calculated using the comparative threshold method ($\Delta\Delta C_T$) and Light Cycler 480 software (Roche Diagnostics).

Histology and light microscopy: To analyze retinal morphology with light microscopy, the eyes were enucleated and fixed in 2.5% glutaraldehyde in 0.1 M cacodylate buffer (pH 7.3) at 4 °C overnight. After fixation, the cornea and the lens were removed, and the eyecup was separated into a superior half and an inferior half by cutting through the optic nerve head. Trimmed tissue was washed in cacodylate buffer, contrasted with osmium tetroxide (1%, 1 h, room temperature), dehydrated by incubation in increasing ethanol concentrations, and embedded in Epon 812. Semithin sections (0.5 µm) were prepared and counterstained with toluidine blue. An Axioplan digitalized microscope (Zeiss Meditec, Jena, Germany) was used to examine the slides. Retinal thickness from the nerve fiber layer to the RPE was measured at fixed distances from the optic nerve head (ONH) using ImageJ (software version 1.43; developed by Wayne Rasband, National Institutes of Health, Bethesda, MD; available NIH).

Immunofluorescence on retinal cryosections: For immunofluorescence, the eyes were enucleated and fixed in 4% paraformaldehyde (PFA) at 4 °C overnight. The cornea and the lens were removed, and the eyecups were incubated in 30% sucrose in phosphate buffered saline (PBS; 1X; 137 mM NaCl, 2.7 mM KCl, 81 mM Na_2HPO_4, 19 mM NaH_2PO_4, pH 7.4) for cryoprotection until the tissue sunk to the bottom of the tube. The tissue was then embedded in tissue cryoprotective medium (catalogue number: 14,020,108,926 Leica Microsystems Nussloch, Nussloch, Germany) and rapidly frozen in a 2-methylbutane bath cooled with liquid nitrogen. Twelve-micrometer-thick sections were cut through the optic nerve head on a Cryostat (Leica), air-dried, and stored at −80 °C until further use. Sections on slides were incubated with blocking solution (3% horse serum in PBS/0.3% Triton X-100) for 1 h at room temperature. Primary antibodies were applied in blocking solution overnight at 4 °C (Table 3). The slides were washed three times with PBS and incubated with Cy2- or Cy3-conjugated secondary antibodies (Jackson ImmunoResesarch, Soham, UK) in blocking solution (dilution 1:500) for 1 h at room temperature. To stain the blood vessels, cryosections were incubated overnight at 4 °C with *G. simplicifolia* isolectin IB_4-Alexa 594 (1:200; catalogue number: I21413; Invitrogen, Basel, Switzerland) in blocking solution. After three washing steps in PBS, the cell nuclei were stained with 4',6-diamidino-2-phenylindole dihydrochloride (DAPI), and the slides were mounted with antifade medium (10% Mowiol 4–88 (vol/vol); Calbiochem, San Diego, CA) in 100 mM Tris (pH 8.5), 25% glycerol (wt/vol), and 0.1% 1,4-diazabicyclo [2.2.2] octane [DABCO]). Immunofluorescently labeled proteins were visualized using an Axioplan fluorescence microscope (Zeiss).

Staining of blood vessels on retinal flatmounts: Eyes were enucleated and incubated in 2% PFA in PBS for 5 min. Subsequently, the cornea and the lens were removed, and the retina was carefully separated from the eyecup. The retina was cut into a "clover-leaf" shape, fixed in methanol (−20 °C), and post-fixed in 4% PFA in PBS for 10 min. The flatmounted retinas were washed briefly with PBS and placed in blocking solution (1% fetal calf serum, 0.1% Triton X-100 in PBS) for 1 h. The retinas were incubated overnight at 4 °C with *G. simplicifolia* isolectin IB_4-Alexa 594 (1:100, catalogue number: I21413; Invitrogen) in blocking solution. The retinal flatmounts were washed with PBS and mounted using antifade medium (see above). Imaging was performed using a digitalized light microscope (Axiovision, Zeiss).

Fluorescein angiography: The mice pupils were dilated with 1% Cyclogyl (Alcon, Cham, Switzerland) and 5% phenylephrine (Ciba Vision, Niederwangen, Switzerland) 1 h before angiography. Mice were anaesthetized with 2.2 µl/g bodyweight of a ketamine/xylazine mix (51/6 mix, subcutaneous injection) 5–10 min before angiography. Eyes were kept moisturized with hydroxypropylmethylcellulose (Methocel 2%, Omnivision, Puchheim, Germany). For fluorescein angiography, 50 µl of 0.2% fluorescein solution (AK Fluor, Akorn, Lake Forest, IL) were injected intraperitoneally, and the retinal vasculature was analyzed with the Micron III retinal imaging system (Phoenix Research Labs, Pleasanton, CA).

Electroretinography: Electroretinograms (ERGs) were recorded according to a previously described procedure [32,33]. The ERG equipment consisted of a Ganzfeld bowl, a direct current amplifier, and a PC-based control and recording unit (LKC UTAS-E 3000, LKC Technologies, Hellendorn, the Netherlands). Mice were dark adapted overnight and

Table 2. Primers used for semiquantitative real-time PCR.

Gene	Forward primer	Reverse primer	Annealing temperature (°C)	Product size (bp)
Actb	CGACATGGAGAAGATCTGGC	CAACGGCTCCGGCATGTGC	62	153
Apaf1	TGAGTACGTGGCATTCGGAG	TGTCTGCCAATTCCATACCTGA	60	184
Bcl2	TGCACCTGACGCCCTTCAC	AGACAGCCAGGAGAAATCAAACAG	62	293
Bcl2l1(BclXL)	GCGGCTGGGACACTTTTGTGG	TGAGCCCAGCAGAACCACACC	60	128
Bdnf	CACTGAGTCTCCAGGACAGC	GTCAGACCTCTCGAACCTGC	60	223
Casp1	GGCAGGAATTCTGGAGCTTCAA	GTCAGTCCTGGAAATGTGCC	60	138
Csf2rb (bCR)	ACTACTACTCCTTCCGGCCA	AGCTGATGCTGACGTTCTTG	62	102
Epo	GCCCTGCTAGCCAATTCC	GCCCTGCTAGCCAATTCC	60	128
EpoR	GTCCTCATCTCGCTGTTGCT	CAGGCCAGATCTTCTGCTG	62	76
Gfap	CCACCAAACTGGCTGATGTCTAC	TTCTCTCCAAATCCACACGAGC	62	240
Gnat1	GAGGATGCTGAGAAGGATGC	TGAATGTTGAGCGTGGTCAT	58	209
Gnat2	GCATCAGTGCTGAGGACAAA	CTAGGCACTCTTCGGGTGAG	58	192
Pou4f1 (Brn3a)	CGCCGCTGCAGAGCAACCTCTT	TGGTACGTGGCGTCCGGCTT	60	130
Rho	CTTCACCTGGATCATGGCGTT	TTCGTTGTTGACCTCAGGCTTG	62	130
sEpoR	TGAAGTGGACGTGTCGGCAG	GGAACTAGGGCCTCACCGCT	60	216
Vsx2 (Chx10)	CCAGAAGACAGGATACAGGTG	GGCTCCATAGAGACCATACT	62	111

Table 3. Antibodies for immunofluorescence on retinal cryosections.

Protein	Host	Supplier	Cat-nr	Dilution
CALB1	rabbit	Chemicon, Billerica, MA	1778	1:500
CALB2	rabbit	Chemicon, Billerica, MA	5054	1:1000
GFAP	mouse	Sigma, St. Louis, MO	G3893	1:500
GNAT1	rabbit	Santa Cruz Biotechnology; Santa Cruz, CA	sc-389	1:500
GNAT2	rabbit	Santa Cruz Biotechnology; Santa Cruz, CA	sc-390	1:500
GLUL (GS)	mouse	Millipore, Billerica, MA	B302	1:500
PKCA	rabbit	Sigma, St. Louis, MO	4334	1:1000
POU4F1 (BRN3A)	mouse	Chemicon, Billerica, MA	1585	1:100
RPE65	rabbit	Pineda Antibodies, Berlin, Germany	Pin-5	1:500
VSX2 (CHX10)	rabbit	generous gift of C. Cepko, Harvard University, MA	-	1:500

anesthetized with ketamine (66.7 mg/kg bodyweight) and xylazine (11.7 mg/kg bodyweight). The pupils were dilated, and single-flash ERG responses were obtained under dark-adapted (scotopic) and light-adapted (photopic) conditions. Light adaptation was accomplished with a background illumination of 30 cd/m^2 starting 5 min before recording. Single white-flash stimulus intensity ranged from –3.7 to 1.9 log cd · s/m^2 under scotopic and from –0.6 to 2.9 log cd · s/m^2 under photopic conditions, divided into ten and eight steps, respectively. Ten responses were averaged with an interstimulus interval (ISI) of either 4.95 s (for –3.7, –3, –2.6, –2, −1.6, –1, –0.6, −0.02, 0.4, and 0.9 log (cd · s/m^2)) or 16.95 s (for 1.4, 1.9, 2.4, and 2.9 log (cd · s/m^2)).

Laser capture microdissection: The eyes were enucleated, immediately embedded in tissue freezing medium (catalogue number: 14,020,108,926; Leica Microsystems Nussloch), and frozen in a 2-methylbutane bath cooled with liquid nitrogen. Retinal sections (20 µm) were fixed (5 min in acetone), air dried (5 min), and dehydrated (30 s in 100% ethanol, 5 min in xylene). Microdissection was performed using an Arcturus XT Laser capture device (Molecular Devices, Sunnyvale, CA). RNA was isolated using the Arcturus kit for RNA isolation (catalogue number: KIT0204; Molecular Devices) according to the manufacturer's directions including a DNase treatment to digest residual genomic DNA. Equal amounts of RNA were used for reverse transcription using oligo(dT) and M-MLV reverse transcriptase (Promega).

Hypoxic exposure: The mice were exposed to reduced oxygen levels in a hypoxic chamber (In Vivo cabinet Model 30; Coy Laboratory Products, Grass Lake, MI) equipped with an oxygen controller (Coy Laboratory Products). During hypoxia, mice had access to food and water ad libitum. By altering the O_2:N_2 ratio, oxygen levels were reduced to the desired concentration in 2% steps over 1 h. Mice were kept at 7% O_2 for 6 h. To analyze the gene and protein expression, the retinas were isolated immediately after the hypoxic period and processed for further analysis. To investigate the retinal morphology, the eyes were enucleated 12 days after hypoxic exposure.

Statistical analysis: Statistical analysis was performed using Prism 4.0 software (GraphPad, San Diego, CA). All data are presented as mean ± standard deviation (SD). The number of samples (n) used for individual experiments is given in the figure legends. Statistical differences of means were calculated using the Student *t* test. Differences with p values below 0.05 were considered significant.

RESULTS

Expression of Epo and *EpoR* isoforms in the retina: *EpoR* expression is elevated in the embryonic brain and decreases into adulthood [22]. A similar situation may be present in the retina. Thus, we analyzed the expression profile of *Epo* and *EpoR* in the newborn and adult retinas of C57BL/6 wild-type mice with semiquantitative real-time PCR. *Epo* was expressed in the newborn retina as early as P3 (Figure 1A). Starting at P10, the expression levels increased by about two- to threefold, reaching more or less steady-state levels in the adult retina (Figure 1A). Similarly, the mRNA levels of *EpoR* were maintained at moderately low levels up to P10, the time point when expression increased by sevenfold to reach a 14-fold increase at 6 months of age (Figure 1B). The *EpoR* gene can be expressed through alternative splicing as a membrane-bound (referred to as "*EpoR*" in the text) and a soluble isoform (soluble *EpoR (sEpoR))*, which encodes for the extracellular domain of EPOR [34-36]. The expression of this isoform has not yet been reported in the retina. To measure the expression of *EpoR* and *sEpoR*, we designed primers specific to each isoform (Appendix 1). Interestingly,

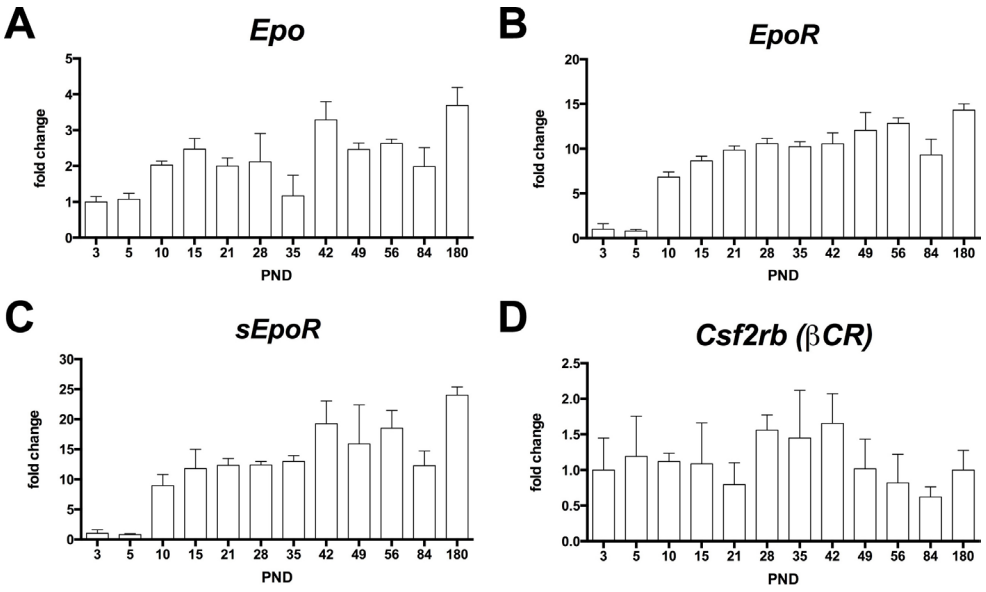

Figure 1. Gene expression profile in the retinas of wild-type mice. Relative expression of erythropoietin *(Epo*; **A**), erythropoietin receptor *(EpoR*; **B**), soluble erythropoietin receptor *(sEpoR*; **C**), and beta common receptor (*Csf2rb* (*βCR*); **D**) as measured with semiquantitative real-time PCR on cDNA samples prepared from the total retinas of the C57BL/6 mice at the postnatal days as indicated. All values were normalized to *actin beta* (*Actb*), and the value at P3 was set to 1. Shown are the mean ± standard deviation (SD) of n = 3 animals.

the expression profile of *sEpoR* was similar to the membrane-bound isoform; that is, it was detectable at low levels up to P10, the time point when expression increased about tenfold and reached approximately 20-fold higher levels in the adult retina (Figure 1C). The EPOR not only forms homo-oligomers but has also been suggested to form hetero-oligomers with the beta common receptor (*Csf2rb* (*βCR*)) [37,38]. In contrast to *EpoR*, expression of *Csf2rb* (*βCR*) remained at steady-state levels in the retina throughout the analyzed period (Figure 1D).

In addition to elucidating the temporal expression profile of *EpoR,* we also analyzed the spatial expression pattern in the retinal tissue to test *EpoR* expression in specific retinal layers. For this purpose, we isolated individual layers (the outer nuclear layer [ONL], the inner nuclear layer [INL], the ganglion cell layer [GCL]) of 12-week-old $EpoR^{flox(flox}$ mice by laser capture microdissection. Analysis of the expression of marker genes for the individual retinal layers showed high purity of the isolated tissue with only a little cross contamination (Appendix 2). *EpoR* transcripts were detected mainly in the GCL and the INL, with markedly lower levels in the ONL, thus suggesting low expression of *EpoR* in photoreceptors (Figure 2).

Knockdown of EpoR in rod photoreceptors or in cells of the retinal periphery has no effect on their development, function, and survival: To explore the possible functions of endogenous EPO-EPOR signaling in the retina, we generated two mouse strains bearing a knockdown of *EpoR* in specific retinal cell populations. We ablated *loxP*-flanked exons 1–4 of the *EpoR* genomic sequence either in rod photoreceptors, by generating $EpoR^{flox/flox}$*;Opn-Cre* mice, or in an assorted population of neurons and glia of the retinal periphery by generating *EpoR*-$^{flox/flox}$*;α-Cre* mice. Note that the lack of exons 1–4 affects the expression of not only *EpoR* but also *sEpoR* (Appendix 1).

By using reporter mouse lines [30,39], we assessed the specificity and localization of CRE-mediated recombination.

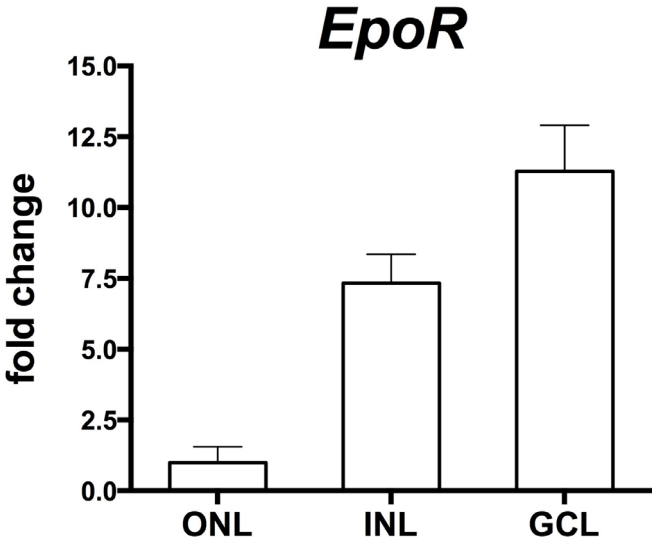

Figure 2. Expression of *EpoR* in the retinal nuclear layers. Semi-quantitative real-time PCR after laser capture microdissection showed relative *EpoR* mRNA levels in the different retinal layers (as indicated) of the $EpoR^{flox/flox}$ control mice. Values were normalized to actin beta (*Actb*) and expressed relative to the value in the ONL, which was set to 1. Shown are the mean ± standard deviation (SD) of at least two mice amplified in duplicate. ONL, outer nuclear layer; INL, inner nuclear layer; GCL, ganglion cell layer.

Although *Opn-Cre*-mediated recombination was specific for the ONL, expression of CRE was patchy and detected in approximately 40% of the total rod population (qualitative estimation) as previously reported [31]. CRE-mediated recombination in the *α-Cre* mouse was detected in a mixed cell population of the retinal periphery and a smaller subset of cells in the central retina (Appendix 3 [40]). Immunostaining with antibodies specific for different retinal cells suggested CRE activity in the Müller glia cells, rod photoreceptors, and horizontal, amacrine, and a subset of ganglion cells (Appendix 3). Whereas in *Opn-Cre* mice, recombination of floxed sequences was maximal only around 10 weeks of age (not shown), CRE activity in *α-Cre* mice showed early onset at E10.5 [41].

At the genomic level, *Opn-Cre* and *α-Cre* successfully deleted *loxP*-flanked exons 1–4 in the *EpoR* gene as evidenced by the appearance of a 220 bp fragment (Figure 3A) that was amplified from recombined genomic DNA when the respective specific primers for PCR were used (Table 1) [23]. To assess the knockdown at the mRNA level, we performed semiquantitative real-time PCR on the total retinal RNA. A statistically significant ($p<0.05$) 35% decrease in *EpoR* mRNA expression was measured in the retinas of the $EpoR^{flox/flox}$;*α-Cre* mice (Figure 3B). However, the decrease in *EpoR* mRNA was not significant in the $EpoR^{flox/flox}$;*Opn-Cre* mice at P84. This was unexpected, but since the total retinal RNA was used for analysis, the effect of a cell-specific knockout may have been masked by cells that did not undergo recombination, especially if those cells (e.g., in the INL and the GCL) expressed the gene at much higher levels (Figure 2). Consequently, we isolated RNA from individual retinal nuclear layers (the ONL, INL, GCL) separated by laser capture microdissection. Amplification of specific marker genes for each nuclear layer suggested high purity of the isolated layers (Appendix 2). Gene expression analysis showed an *EpoR* expression level in the ONL of $EpoR^{flox/flox}$;*Opn-Cre* mice that was reduced by about 35% compared to the control littermates, even though the knockdown did not reach statistical significance (Figure 3C). This efficiency of *EpoR* knockdown was similar to the fraction of photoreceptors that express *Cre* recombinase in the *Opn-Cre* mouse retina [29,31]. Although the knockdown efficiency was not high when calculated on the level of the total retina or the ONL (cells without active CRE still express *EpoR*), most *Cre*-expressing cells (e.g., 30–40% of rods) should have recombined floxed sequences on both alleles leading to many cells harboring a complete knockout and therefore lacking the EPOR protein. Due to the lack of reliable antibodies [42,43], the EPOR protein levels and tissue distribution were not analyzed with western blotting or immunofluorescence.

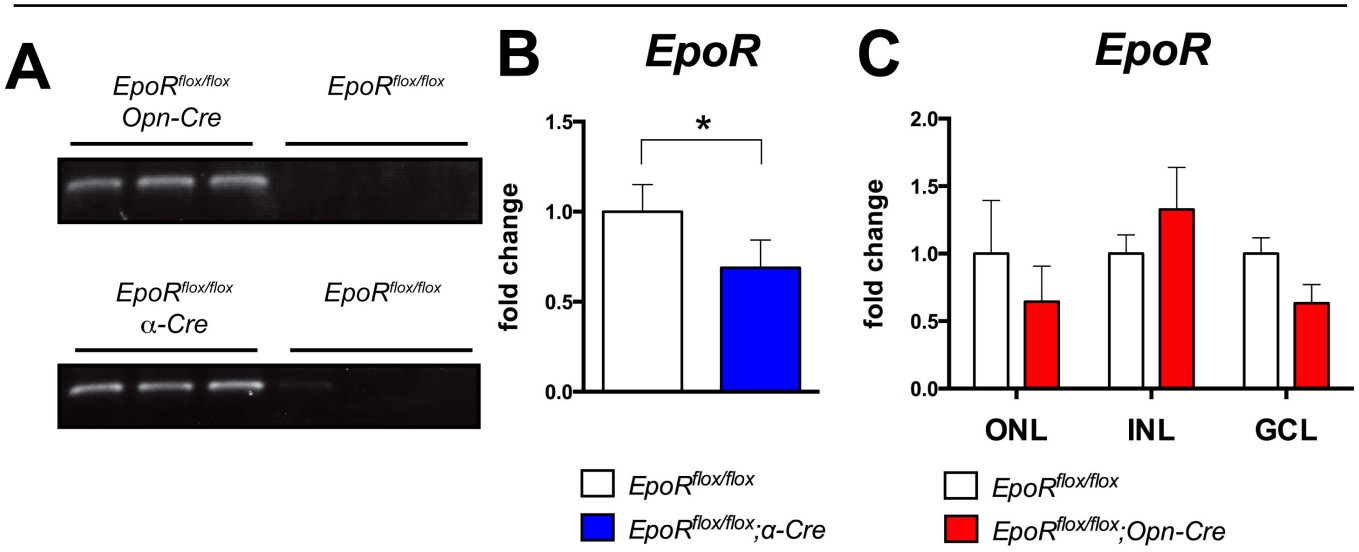

Figure 3. Knockdown of *EpoR* in the $EpoR^{flox/flox}$;*Opn-Cre* and $EpoR^{flox/flox}$;*α-Cre* retinas. A: PCR amplification of genomic DNA isolated from the retinas of $EpoR^{flox/flox}$, $EpoR^{flox/flox}$;*Opn-Cre,* and $EpoR^{flox/flox}$; *α-Cre* mice at P84 (n = 3). CRE-mediated recombination resulted in the amplification of a 220 bp fragment. **B**: Semiquantitative real-time PCR analysis of the expression of *EpoR* in total retinal RNA from the $EpoR^{flox/flox}$;*α-Cre* mice (blue bar) and the $EpoR^{flox/flox}$ mice (white bar) at P84. Values were normalized to *actin beta* (*Actb*), and the $EpoR^{flox/flox}$ values were set to 1. Shown are the mean ± standard deviation (SD) of n = 4 animals. **C**: Semiquantitative real-time PCR analysis of *EpoR* levels in different retinal layers separated by laser capture microdissection from the $EpoR^{flox/flox}$ (white bars) and $EpoR^{flox/flox}$;*Opn-Cre* mice (red bars). Values were normalized to *actin beta* (*Actb*) and expressed relative to the value of $EpoR^{flox/flox}$ mice for each layer, which were set to 1. Shown are the mean ± SD of at least two mice. ONL, outer nuclear layer; INL, inner nuclear layer; GCL, ganglion cell layer. The differences in gene expression levels between the knockdown and control mice were tested for significance using a Student *t* test. *: $p<0.05$.

The absence of EPOR results in increased apoptosis of NPCs and thus affects brain development [22]. Since *α-Cre* mice recombine floxed sequences in embryonic retinal progenitor cells, the absence of or reduced levels of EPOR may lead to developmental defects and thus to morphological alterations in the adult retina. However, histological analysis did not reveal tangible signs of developmental defects, and normal morphology was observed up to 1 year of age in the retinal periphery of the *EpoR*$^{flox/flox}$*;α-Cre* mice (Figure 4A). Similarly, the retina and in particular the photoreceptors of the *EpoR*$^{flox/flox}$*;Opn-Cre* mice showed normal morphology up to 1 year of age (Figure 4A). Analysis of the expression of *rhodopsin* (*Rho*), *guanine nucleotide binding protein, alpha transducin 2* (*Gnat2*), *visual system homeobox 2 Vsx2* (*Chx10*), and *POU domain, class 4, transcription factor 1 Pou4f1* (*Brn3a*) indicated that the number of rods, cones, bipolar cells, and RGCs, respectively, was not affected in the *EpoR* knockdown mice up to 7.5 months of age (Figure 4B,C). The absence of retinal degeneration in both *EpoR* knockdown strains was confirmed with morphometric analysis of retinal thickness in 7.5-month-old mice (Figure 4D). Furthermore, ERG recordings pointed to normal retinal function (Figure 5A,B). Neither the *EpoR*$^{flox/flox}$*;Opn-Cre* mice nor the *EpoR*$^{flox/flox}$*;α-Cre* mice showed significant changes in a- and b-wave amplitudes under scotopic or photopic conditions when compared to the control littermates (Figure 5C–E). Taken together, these results demonstrate that expression of *EpoR* was not necessary for the correct maturation and function of rod photoreceptors and cells in the retinal periphery. In addition, long-term survival of the retinal neurons, including photoreceptors, was not impaired by the absence of EPOR in our knockdown mice.

Lack of the erythropoietin receptor has no influence on retinal cell viability in acute hypoxia: The induction of *Epo* expression under hypoxic conditions suggested that this cytokine may be particularly important for preserving cell viability when oxygen is limited [9,44]. In fact, EPO was shown to support neuronal survival against hypoxia-induced cell death in vitro [45], and in an in vitro model of cerebral ischemia [46]. These findings have been corroborated in vivo in a model of brain ischemia/hypoxia [47]. In line with this notion, neural cells lacking *EpoR* showed increased sensitivity to hypoxia in vitro [22]. To investigate the ability of EPOR to mediate the resistance of retinal cells against hypoxia, we exposed 12-week-old *EpoR* knockdown mice to hypoxia (7% O_2; 6 h) and analyzed the retinal morphology 12 days after the hypoxic exposure to detect potential signs of tissue damage. Qualitative investigation of retinal morphology did not reveal signs of cell loss upon hypoxic exposure in both strains of *EpoR* knockdown mice when compared to the control littermates (Figure 6A, compare to Figure 4A for the retinal morphology of normoxic mice). These qualitative findings were confirmed with morphometric measurements of the retinal thickness, which was comparable to that of the normoxic mice (Figure 6B, compare to Figure 4D for retinal thickness of normoxic mice). Thus, ablation of *EpoR* in the retinal periphery or in rod photoreceptors does not increase retinal susceptibility to acute hypoxia.

Lack of EpoR may alter erythropoietin-erythropoietin receptor signaling in the hypoxic retina: EPOR downstream signaling activates several signal transduction pathways. They may ultimately modulate the transcription of target genes involved in various biologic processes, including cell growth or apoptosis [48]. Genes shown to be influenced by EPO signaling include the antiapoptotic genes B-cell lymphoma 2 (*Bcl2*) and Bcl-2-like 1 (*Bcl2l1* [*BclXL*]) [49,50], the proapoptotic genes caspase 1 (*Casp1*) [19] and apoptotic protease activating-factor 1 (*Apaf1*) [51,52], the neurotrophic factor brain-derived neurotrophic factor (*Bdnf*) [53], and the gliotic response gene glial fibrillary acidic protein (*Gfap*) [54].

To test the influence of *EpoR* knockdowns on EPO-EPOR signaling in the retina, we exposed mice at P84 to a short period of hypoxia (7% O_2, 6 h) and analyzed the gene expression immediately thereafter (Figure 7). As expected, expression of *Epo* was increased in all mouse retinas after this treatment. Expression of *EpoR* was not significantly affected after hypoxia in both knockdown strains. CRE-mediated deletion of exons 1–4 of the *EpoR* gene prevented expression of not only *EpoR* but also *sEpoR* (Appendix 1) [34-36,55]. The expression levels of this isoform were not reduced in the *EpoR*$^{flox/flox}$*;Opn-Cre* retinas when the total retinal RNA was measured. However, *sEpoR* transcripts were significantly ($p<0.001$) reduced by approximately two thirds in the retinas of the *EpoR*$^{flox/flox}$*;α-Cre* mice at P84. In both knockdown mice strains, hypoxia did not influence the expression of *sEpoR*. Importantly, knockdown of *EpoR* did not lead to compensatory upregulation of *Csf2rb (βCR)*. Whereas expression of *Bcl2l1 and Bcl2* was not affected by the lack of EPOR, *Apaf1*, *Casp1*, and *Gfap* were downregulated and the prosurvival factor *Bdnf* was upregulated specifically in the hypoxic retinas (and thus in the presence of the increased EPO) of *EpoR*$^{flox/flox}$*;α-Cre* mice (Figure 7B). This indicates that lack of EPOR influenced the gene expression profile in the hypoxic retinas in ways that suggested reduced expression of stress-related genes and increased expression of prosurvival genes. These results were unexpected since EPO-EPOR signaling is generally accepted to be prosurvival, and thus, lack of EPOR should reduce such signaling (see

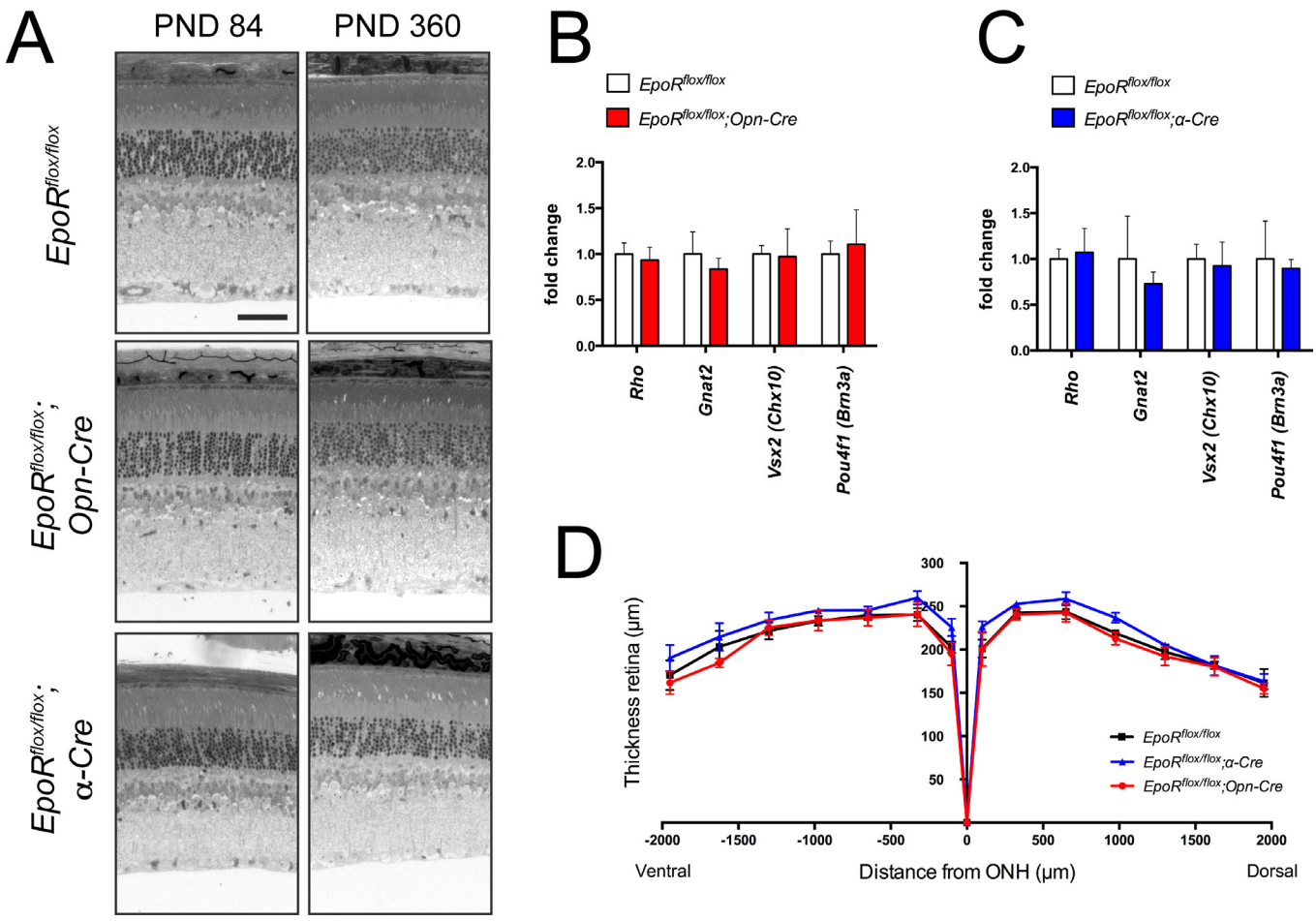

Figure 4. Retinal morphology of *EpoR* knockdown mice. **A**: Retinal morphology of the *EpoR*$^{flox/flox}$, *EpoR*$^{flox/flox}$*;Opn-Cre* and *EpoR*$^{flox/flox}$*;α-Cre* mice at P84 and P360. Shown are representative sections of the central retina (*EpoR*$^{flox/flox}$ *and EpoR*$^{flox/flox}$*;Opn-Cre*) and the peripheral retina (*EpoR*$^{flox/flox}$*;α-Cre*) of at least three animals per time point. Scale bar: 50 µm. **B**, **C**: Relative expression levels of rhodopsin (*Rho*), guanine nucleotide binding protein alpha transducin 2 (*Gnat2*), visual system homeobox 2 (*Vsx2 (Chx10)*), and POU domain, class 4 transcription factor 1 (*Pou4f1 (Brn3a)*) mRNAs as determined with semiquantitative real-time PCR in the total retinas of the *EpoR*$^{flox/flox}$*;Opn-Cre* (**B**, red bars), *EpoR*$^{flox/flox}$*;α-Cre* (**C**, blue bars), and *EpoR*$^{flox/flox}$ control littermates (**B**, **C**, white bars) at 7.5 months of age. Given are the mean ± standard deviation (SD) of n = 4 retinas. Values were normalized to actin beta (*Actb*) and expressed relative to the *EpoR*$^{flox/flox}$ control littermates, in which expression was set to 1. The differences in gene expression levels between the knockdown and control mice at individual time points were tested for significance using a Student *t* test. **D**: Retinal thickness of 7.5-month-old *EpoR*$^{flox/flox}$*;Opn-Cre* mice (red line), *EpoR*$^{flox/flox}$*;α-Cre* mice (blue line), and *EpoR*$^{flox/flox}$ mice (black line). Thickness was measured at 0, 100, 325, 650, 975, 1300, 1625, and 1950 µm from the optic nerve head (ONH) in the dorsal and ventral hemispheres, as indicated. Shown are the mean ± SD of n = 3 animals. The differences in retinal thickness between the knockdown and control mice were tested for significance using a Student *t* test.

the Discussion section). In contrast to the *EpoR*$^{flox/flox}$*;α-Cre* mice, the lack of EPOR in the rods of the *EpoR*$^{flox/flox}$*;Opn-Cre* mice did not lead to detectable changes in the gene expression profile (Figure 7A), suggesting that EPOR signaling may affect the inner retinal layers rather than the photoreceptor layer.

Ablation of EpoR does not inhibit angiogenesis: Since evidence suggests that EPOR signaling is involved in angiogenesis [56], we investigated whether ablation of EPOR in retinal progenitors during development might affect retinal vascular development. Using retinal flatmounts and cross-sections, we did not detect any overt vascular abnormalities in the *EpoR*$^{flox/flox}$*;α-Cre* mice. In particular, the capillary coverage in the retinal periphery was not decreased (Figure 8A), and all three retinal capillary plexi developed properly at their correct location (Figure 8B). Perfusion and stability of the retinal vasculature were also not grossly affected as revealed with fluorescein angiography and the absence of signs of vascular leakage (Figure 8C). As expected, ablation

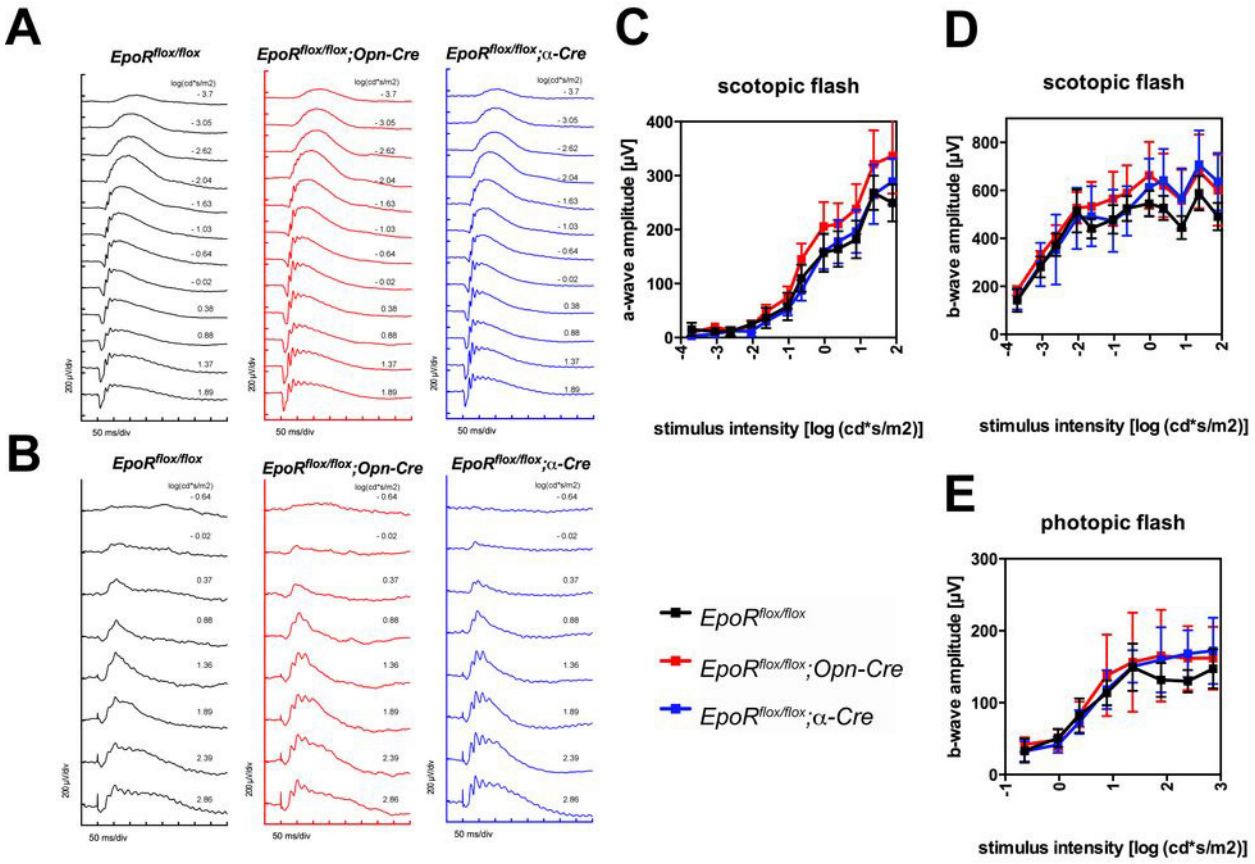

Figure 5. Retinal function in *EpoR* knockdown mice. (**A**) Scotopic and (**B**) photopic electroretinogram (ERG) recordings in the *EpoR*$^{flox/flox}$*;Opn-Cre* and *EpoR*$^{flox/flox}$*;α-Cre* mice and the *EpoR*$^{flox/flox}$ control littermates. (**C**) Scotopic a-wave, (**D**) scotopic b-wave, and (**E**) photopic b-wave amplitudes plotted as a function of light intensity. Shown are the mean ± standard deviation (SD) of n = 3 animals per genotype.

of EPOR in mature rod photoreceptors did not lead to any detectable differences from the wild-type (Figure 8A–C).

DISCUSSION

Elucidating the expression pattern of EPOR in the retina has been the scope of many vision scientists over the past few years, and various studies have used immunohistochemistry to investigate the expression of EPOR. Unfortunately, the commercially available anti-EPOR antibodies have recently been shown to give unreliable results, and thus, caution should be taken when interpreting these studies [42,43]. In the absence of reliable antibodies, the expression of *EpoR* should be analyzed with alternative methods. Colella et al. showed with in situ hybridization that *EpoR* transcripts accumulate at elevated levels in the INL and the GCL [57]. Our data on the expression of *EpoR* mRNA in the different retinal nuclear layers isolated with laser capture microdissection confirm this observation, and most importantly suggest that photoreceptors do not express high levels of *EpoR*. Instead, *EpoR* may be expressed predominantly in the neurons and presumably Müller cells of the inner retina (Figure 2). Interestingly, Chen and coworkers reported that neural progenitors express higher levels of EPOR than mature neurons in the brain [58]. In spite of this, we measured increased retinal expression of *EpoR* starting at P10, a time point when differentiation of RPCs is completed [59] (Figure 1B). Thus, in the retina, mature neurons and glia seemed to express higher levels of *EpoR* compared to the RPCs.

Yu and coworkers showed that *EpoR* null mice have fewer NPCs [22]. Chen et al. made a similar observation in *EpoR* null mice that were rescued with selective *EpoR* expression driven by the endogenous *EpoR* promoter in hematopoietic tissue but not in the brain [58]. This indicates that endogenous EPO-EPOR signaling supports cell viability in the embryonic brain. However, we did not detect any morphological or functional defects that would hint at developmental abnormalities in the retinal periphery of *EpoR*$^{flox/flox}$*;α-Cre* mice (Figure 4A, Figure 5). Together, these observations indicated that endogenous EPO-EPOR signaling is not crucial for RPC survival and development of retinal neurons (RGCs, amacrine,

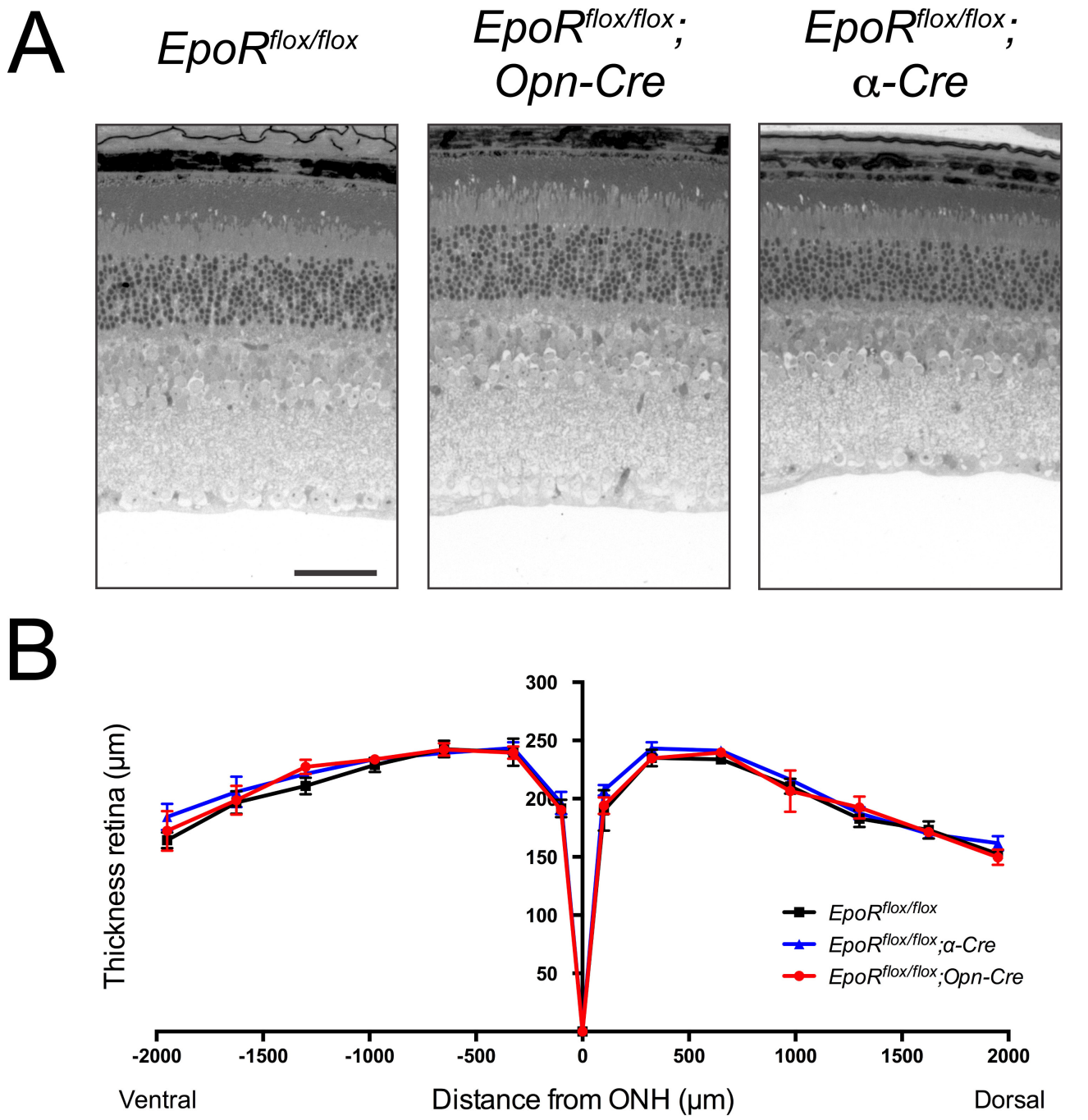

Figure 6. Retinal morphology of *EpoR* knockdown mice exposed to hypoxia. **A**: Retinal morphology of the *EpoR*$^{flox/flox}$, *EpoR*$^{flox/flox}$*;Opn-Cre,* and *EpoR*$^{flox/flox}$*;α-Cre* mice analyzed 12 days after they were exposed to hypoxia (7% O_2, 6 h). Shown are representative sections of the central retina (*EpoR*$^{flox/flox}$ and *EpoR*$^{flox/flox}$*;Opn-Cre* mice) or the peripheral retina (*EpoR*$^{flox/flox}$*;α-Cre* mice) of three animals per time point. Scale bar: 50 µm. **B**: Thickness of the retinas of the *EpoR*$^{flox/flox}$ (black line), *EpoR*$^{flox/flox}$*;Opn-Cre,* (red line), and *EpoR*$^{flox/flox}$*;α-Cre* (blue line) mice. Thickness was measured 12 days after the mice were exposed to hypoxia (7% O_2, 6 h) at 0, 100, 325, 650, 975, 1300, 1625, and 1950 µm from the optic nerve head (ONH) in the dorsal and ventral hemispheres, as indicated. Shown are the mean ± standard deviation (SD); n = 3. The differences in retinal thickness between the knockdown and control mice were tested for significance using a Student *t* test.

horizontal, and photoreceptor cells) and glia (Müller cells), at least not in the retinal periphery. Furthermore, the absence of tangible signs of retinal degeneration in the retinal periphery of 1-year-old *EpoR*$^{flox/flox}$*;α-Cre* retinas suggested that EPOR

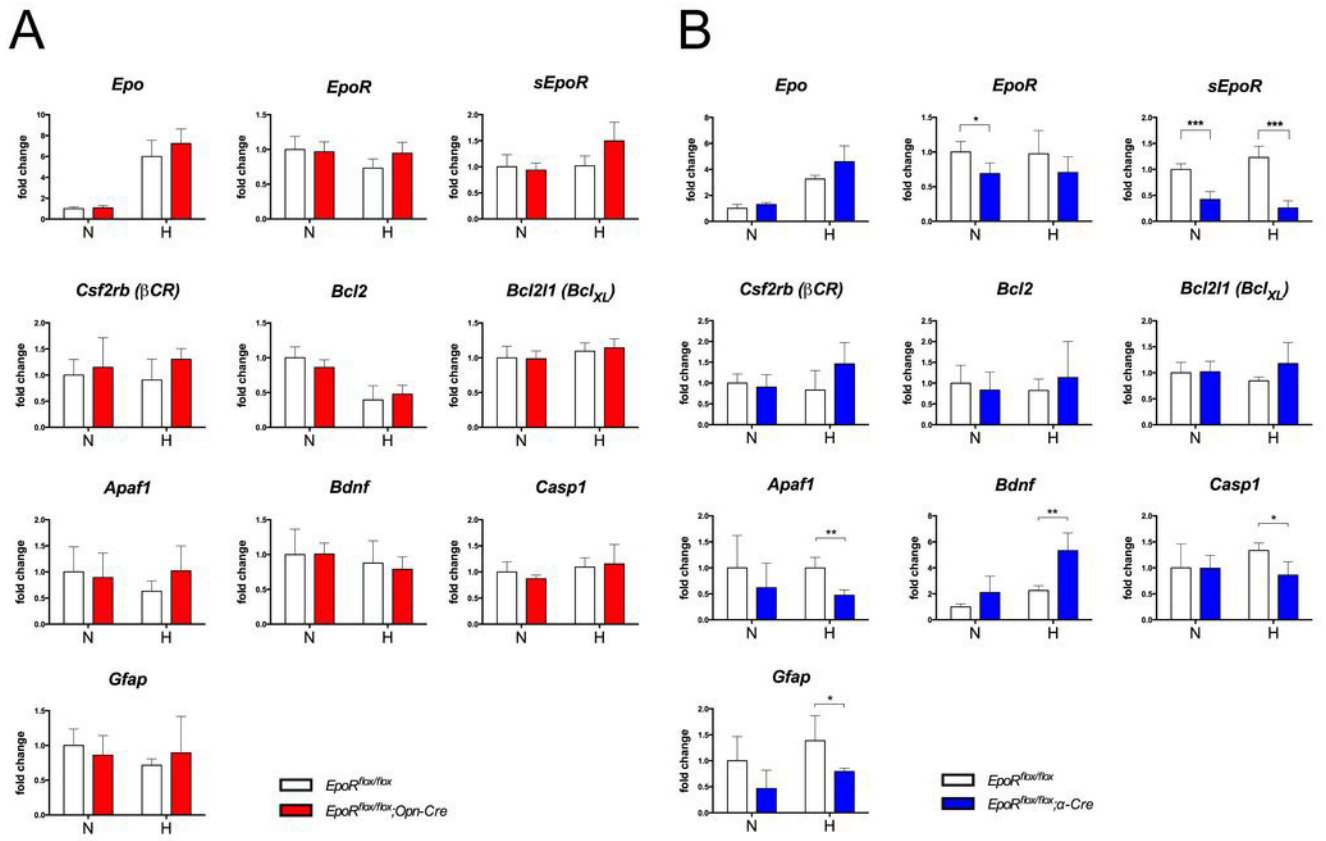

Figure 7. Expression of selected genes in the retinas of *EpoR* knockdown mice. **A**, **B**: Relative quantification of erythropoietin (*Epo*), erythropoietin receptor (*EpoR*), soluble erythropoietin receptor (*sEpoR*), beta common receptor (*Csf2rb (βCR)*), B cell lymphoma 2 (*Bcl2*), Bcl2-like 1 (*Bcl2l1(BclXL)*), apoptotic protease activating factor 1 (*Apaf1*), brain-derived neurotrophic factor (*Bdnf*), caspase 1 (*Casp1*), and glial fibrillary acidic protein (*Gfap*) gene expression in the retinas of the *EpoR*$^{flox/flox}$*;Opn-Cre* (**A**) and the *EpoR*$^{flox/flox}$*;α-Cre* mice (**B**) compared to *EpoR*$^{flox/flox}$ control littermates with real-time PCR. cDNAs were prepared from total retinal RNA isolated at P84. Animals were kept under normoxic conditions (N) or exposed to hypoxia (H, 7% O_2, 6 h) immediately before euthanasia and retina isolation. Given are the mean ± standard deviation (SD) for n = 4 retinas. Values were normalized to *actin beta* (*Actb*) and expressed relative to the *EpoR*$^{flox/flox}$ control littermates under normoxic conditions, which were set to 1. The differences in gene expression levels between the knockdown and control mice at individual time points and conditions were tested for significance using a Student *t* test *: p<0.05; **: p<0.01; ***: p<0.001.

signaling is also not necessary for the survival of retinal cells under non-pathological conditions.

The absence of any detectable consequence of *EpoR* knockdown in rod photoreceptors may be explained by the low expression level of *EpoR* in the ONL (Figure 2). This also suggests that EPOR may not be directly involved in photoreceptor physiology and survival, a conclusion supported by the integrity of the retinal tissue in aging *EpoR*$^{flox/flox}$*;Opn-Cre* mice (Figure 4A).

In addition to the membrane-bound isoform, we also detected retinal expression of *sEpoR,* as has been previously reported for the brain [60]. Expression of *sEpoR* in the postnatal retinas of wild-type mice followed a profile remarkably similar to the membrane-bound isoform of *EpoR* (Figure 1C). This is interesting regarding the proposed function of sEPOR. Based on a study published by Soliz et al., sEPOR may act as a negative regulator of EPO signaling. The soluble isoform consists of the extracellular domain and binds EPO, therefore sequestering the cytokine and preventing it from binding to the membrane-bound EPOR, and thus from activating intracellular signaling cascades [60,61]. Soluble receptors frequently modulate cytokine signaling by stabilizing the cytokine, changing its tissue concentration, or modifying its interaction with the membrane-bound receptor [62,63]. For example, intravitreal injection of sEPOR in a rat model of retinal detachment led to increased photoreceptor apoptosis [64], and coapplication of EPO and sEPOR blocked the protective effects of EPO in an in vitro model of cerebral ischemia [46]. The soluble form of EPOR could have a similar function in the retina and abrogate EPO-EPOR signaling by

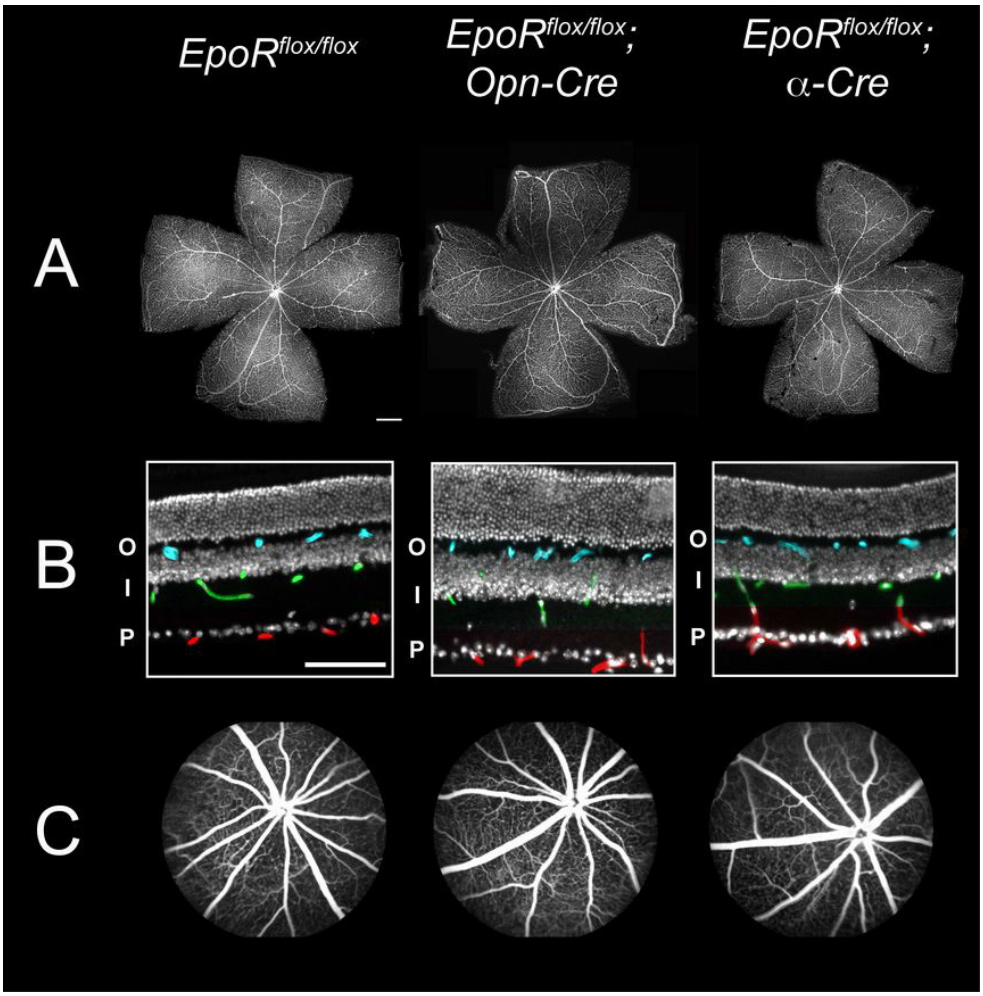

Figure 8. Retinal vasculature and vascular perfusion in the *EpoR* knockdown mice. **A**: Retinal flatmounts of *EpoR*$^{flox/flox}$ and *EpoR*$^{flox/flox}$;*Opn-Cre* littermates at P84 and of the *EpoR*$^{flox/flox}$;α-*Cre* mice at P30. Vessels were stained with isolectin IB_4 coupled to Alexa 594. Shown are representative flatmounts of three animals per genotype. Scale bar: 500 µm. **B**: Staining of blood vessels on retinal cryosections (isolectin IB_4, coupled to Alexa 594) in the *EpoR*$^{flox/flox}$, *EpoR*$^{flox/flox}$;*Opn-Cre*, and *EpoR*$^{flox/flox}$;*α-Cre* mouse retinas at P84. Vessels were highlighted with artificial coloring (primary plexus (P): red; intermediate plexus (I): green; outer plexus (O): blue). Cell nuclei were stained with 4',6-diamidino-2-phenylindole dihydrochloride (DAPI) (white). Scale bar: 100 µm. **C**: Fluorescein angiography of the *EpoR*$^{flox/flox}$, *EpoR*$^{flox/flox}$;*Opn-Cre*, and *EpoR*$^{flox/flox}$;α-*Cre* mouse retinas at P84 performed with Micron III imaging. Shown are representative images of three animals per genotype.

sequestering endogenous EPO. As a consequence, EPO-EPOR signaling in the retina may occur only under conditions where EPO protein levels are elevated, such as under hypoxia or upon exogenous EPO applications. Intriguingly, the expression of *sEpoR* in the brain and plasma has been reported to be reduced in hypoxia [60,65], thus allowing advanced modulation of the EPO response under these conditions. However, similar downregulation of *sEpoR* expression was not observed in the retina after acute hypoxia (Figure 7). Either the hypoxic period was too short to cause downregulation of *sEpoR*, or regulation of sEPOR synthesis is not controlled at the transcriptional level in the retina.

To understand the regulatory function of sEPOR, the retinal cell populations that express each isoform must be identified. Ablation of *EpoR* in the retinal periphery of the *EpoR*$^{flox/flox}$*;α-Cre* mice caused a strong and significant decrease in the *sEpoR* transcript levels of about two thirds, whereas *EpoR* expression decreased only by roughly one third (Figures 3B, 7B). Based on this observation, we deduced that the population of cells that was CRE-positive in the *EpoR*$^{flox/flox}$*;α-Cre* retina was expressing elevated levels of *sEpoR* in the wild-type retina under normal conditions. Due to the heterogeneous population of cells undergoing CRE-mediated recombination in the *α-Cre* mouse retina, it is difficult to make any assumptions about the identity of the retinal cell types that express *sEpoR*. Nevertheless, based on the unaltered expression of *sEpoR* in the retinas of the *EpoR*$^{flox/flox}$*;Opn-Cre* mice (Figure 7A), we suggest that rod photoreceptors do not significantly participate in the secretion of sEPOR.

We did not measure significant changes in gene expression in the normoxic or hypoxic retinas of the *EpoR*$^{flox/flox}$*;Opn-Cre* mice (Figure 7A). The relatively low expression of *EpoR* in the ONL of the *EpoR*$^{flox/flox}$*;Opn-Cre* mice could explain this observation. The gene expression profile in the *EpoR*$^{flox/flox}$*;α-Cre* knockdown mice, however, gave unexpected results. Several genes (*Apaf1*, *Casp1*, *Gfap*) that had been expected to show increased expression in the absence

of EPOR were in fact expressed at lower levels in the hypoxic retinas of these mice. The opposite was true for genes that had been expected to be downregulated in *EpoR*$^{flox/flox}$*;α-Cre* mice (*Bdnf*; Figure 7B). The reduced expression of *sEpoR* in the retinas of the *EpoR*$^{flox/flox}$*;α-Cre* mice may explain these surprising results. Cells not affected by *EpoR* ablation (cells that do not express CRE) could show increased EPO-EPOR signaling due to potentially reduced levels of extracellular sEPOR. The diminished presence of sEPOR would result in reduced sequestration of EPO, thus allowing augmented activation of the membrane-bound EPOR and downstream target genes. However, this hypothesis is speculative and clearly needs additional support with experimental data. Analysis of gene and protein expression in mice with efficient knockdown of *EpoR* in a single retinal cell type would be needed to specifically determine the influence of EPO-EPOR signaling on retinal physiology. Alternatively, the consequences of the absence of EPOR in the retina could be studied in *EpoR* null mice that are rescued by selective *EpoR* expression in hematopoietic tissue but not in the neural cells [58].

The angiogenic activity of EPO during development may be related to the stimulation of endothelial progenitor cell mobilization or proliferation [66]. Expression of *EpoR* has been detected in various types of vascular endothelial cells [67], and it is therefore assumed that the angiogenic activities of EPO are directly mediated through binding to EPOR expressed on the surface of vascular endothelial cells. In the *α-Cre* mouse, *Cre* recombinase is not expressed in retinal vascular endothelial cells [68]. Therefore, it may not be surprising that the retinal vasculature did not show any signs of developmental defects. Nevertheless, we also ruled out indirect effects suggesting that the EPO-EPOR system in RGCs, amacrine, horizontal, and Müller cells does not significantly contribute to the development of the vasculature in the retinal periphery. However, it would be of great interest to specifically ablate *EpoR* in vascular cells and analyze the retinal vasculature under these conditions.

Based on data presented in this study, we conclude that EPOR is not required for the development and long-term survival of retinal neurons (RGCs, amacrine, horizontal, and rod photoreceptor cells) and glia (Müller cells) in the retinal periphery. The parallel longitudinal expression profile of *EpoR* and s*EpoR* in the postnatal retina suggests that EPO-EPOR signaling may not be constantly activated in this neural tissue.

APPENDIX 1. SPECIFICITY OF PRIMERS FOR ERYTHROPOIETIN RECEPTOR *(EPOR)* ISOFORMS.

Schematic diagram representing the mRNA structure (exon 4 to 6 are shown) of *EpoR* and soluble *EpoR (sEpoR)*. Primers specific to *EpoR* bind to exon 5 (*EpoR* forward) and to the exon 5 – exon 6 junction (*EpoR* reverse). Primers specific to *sEpoR* bind to exon 4 (*sEpoR* forward) and to the exon 5 – exon 5a junction (*sEpoR* reverse). Exon 5a corresponds to intron 5, which is retained in *sEpoR* mRNA and contains an in-frame stop codon that results in the translation of EPOR lacking the transmembrane and cytosolic domains [69]. To access the data, click or select the words "Appendix 1."

APPENDIX 2. ASSESSMENT OF CROSS-CONTAMINATION BY SEMIQUANTITATIVE REAL-TIME PCR OF RETINAL LAYERS ISOLATED BY LASER CAPTURE MICRODISSECTION.

(A) POU domain, class 4, transcription factor 1 *(Pou4f1 (Brn3a))*, a marker for the ganglion cell layer. **(B)** visual system homeobox 2 *(Vsx2 (Chx10))*, a marker for the inner nuclear layer. **(C)** Guanine nucleotide binding protein, alpha transducin 1 *(Gnat1)*, a marker for the outer nuclear layer. Tissue was isolated from of *EpoR*$^{flox/flox}$*;Opn-Cre*, and *EpoR*-$^{flox/flox}$ control littermates. Values were normalized to actin beta *(Actb)* and expressed relatively to the value of *EpoR*$^{flox/flox}$ in the ONL, which was set to 1. Shown are mean values ± SD of at least 2 different mice. ONL, outer nuclear layer; INL, inner nuclear layer; GCL, ganglion cell layer. To access the data, click or select the words "Appendix 2."

APPENDIX 3. LOCALIZATION OF CRE ACTIVITY IN THE RETINA OF *AI6;A-CRE* REPORTER MICE.

(A) Retinal cryosection of *Ai6;α-Cre* mice (cut naso-temporal) at post-natal day (PND) 15. ZSGREEN fluorescence (green) indicates cells that underwent CRE mediated recombination. Inset (A1) shows a higher magnification of the transition zone between central and peripheral retina. Scale bars: 200 µm and 50 µm (inset). (B) Identification of CRE-expressing retinal cells by the co-localization of ZSGREEN and different cell markers in *Ai6;α-Cre* mice at PND 15. Shown are retinal cryosections presenting native ZSGREEN fluorescence after CRE-mediated recombination (green) and immunostainings for different retinal cell markers (red) as indicated. POU domain, class 4, transcription factor 1 (POU4F1 (BRN3A)) for retinal ganglion cells (RGCs); calbindin 1 (CALB1) for horizontal cells and a subset of amacrine cells; calbindin 2

(CALB2) for amacrine cells and a subset of ganglion cells; glutamate-ammonia ligase (GLUL (GS)) for Müller cells; glial fibrillary acidic protein (GFAP) for astrocytes and activated Müller cells; visual system homeobox 2 (VSX2 (CHX10)) for bipolar cells; protein kinase C alpha (PKCA) for rod bipolar cells; retinal pigment epithelium-specific 65 kDa protein (RPE65) for the retinal pigment epithelium. Scale bar: 100 µm. RPE: retinal pigment epithelium; ONL: outer nuclear layer; OPL: outer plexiform layer; INL: inner nuclear layer; IPL: inner plexiform layer; GCL: ganglion cell layer; D: dorsal; V: ventral. To access the data, click or select the words "Appendix 3."

ACKNOWLEDGMENTS

The authors thank Coni Imsand for outstanding technical assistance with retinal histology, Christel Beck and Andrea Gubler for genotyping. This work was supported by the Swiss National Science Foundation (31003A_133043).

REFERENCES

1. Krantz SB. Erythropoietin. Blood 1991; 77:419-34. [PMID: 1991159].
2. Koury ST, Bondurant MC, Semenza GL, Koury MJ. The use of in situ hybridization to study erythropoietin gene expression in murine kidney and liver. Microsc Res Tech 1993; 25:29-39. [PMID: 8353306].
3. Koury MJ, Bondurant MC. Maintenance by erythropoietin of viability and maturation of murine erythroid precursor cells. J Cell Physiol 1988; 137:65-74. [PMID: 2459142].
4. Bondurant MC, Koury MJ. Anemia induces accumulation of erythropoietin mRNA in the kidney and liver. Mol Cell Biol 1986; 6:2731-3. [PMID: 3785209].
5. Jelkmann W. Molecular biology of erythropoietin. Intern Med 2004; 43:649-59. [PMID: 15468961].
6. Fried W, Kilbridge T, Krantz S, McDonald TP, Lange RD. Studies on extrarenal erythropoietin. J Lab Clin Med 1969; 73:244-8. [PMID: 5764021].
7. Fandrey J. Oxygen-dependent and tissue-specific regulation of erythropoietin gene expression. Am J Physiol Regul Integr Comp Physiol 2004; 286:R977-88. [PMID: 15142852].
8. Farrell F, Lee A. The erythropoietin receptor and its expression in tumor cells and other tissues. Oncologist 2004; 9:Suppl 518-30. [PMID: 15591419].
9. Juul SE, Yachnis AT, Christensen RD. Tissue distribution of erythropoietin and erythropoietin receptor in the developing human fetus. Early Hum Dev 1998; 52:235-49. [PMID: 9808074].
10. Xie Z, Wu X, Qiu Q, Gong Y, Song Y, Gu Q, Li C. Expression pattern of erythropoietin and erythropoietin receptor in experimental model of retinal detachment. Curr Eye Res 2007; 32:757-64. [PMID: 17882708].
11. Patel NS, Sharples EJ, Cuzzocrea S, Chatterjee PK, Britti D, Yaqoob MM, Thiemermann C. Pretreatment with EPO reduces the injury and dysfunction caused by ischemia/reperfusion in the mouse kidney in vivo. Kidney Int 2004; 66:983-9. [PMID: 15327391].
12. Parsa CJ, Matsumoto A, Kim J, Riel RU, Pascal LS, Walton GB, Thompson RB, Petrofski JA, Annex BH, Stamler JS, Koch WJ. A novel protective effect of erythropoietin in the infarcted heart. J Clin Invest 2003; 112:999-1007. [PMID: 14523037].
13. Cai Z, Manalo DJ, Wei G, Rodriguez ER, Fox-Talbot K, Lu H, Zweier JL, Semenza GL. Hearts from rodents exposed to intermittent hypoxia or erythropoietin are protected against ischemia-reperfusion injury. Circulation 2003; 108:79-85. [PMID: 12796124].
14. Brines ML, Ghezzi P, Keenan S, Agnello D, de Lanerolle NC, Cerami C, Itri LM, Cerami A. Erythropoietin crosses the blood-brain barrier to protect against experimental brain injury. Proc Natl Acad Sci USA 2000; 97:10526-31. [PMID: 10984541].
15. Fu QL, Wu W, Wang H, Li X, Lee VW, So KF. Up-regulated endogenous erythropoietin/erythropoietin receptor system and exogenous erythropoietin rescue retinal ganglion cells after chronic ocular hypertension. Cell Mol Neurobiol 2008; 28:317-29. [PMID: 17554621].
16. Weishaupt JH, Rohde G, Polking E, Siren AL, Ehrenreich H, Bahr M. Effect of erythropoietin axotomy-induced apoptosis in rat retinal ganglion cells. Invest Ophthalmol Vis Sci 2004; 45:1514-22. [PMID: 15111610].
17. Tsai JC, Wu L, Worgul B, Forbes M, Cao J. Intravitreal administration of erythropoietin and preservation of retinal ganglion cells in an experimental rat model of glaucoma. Curr Eye Res 2005; 30:1025-31. [PMID: 16282136].
18. Zhong L, Bradley J, Schubert W, Ahmed E, Adamis AP, Shima DT, Robinson GS, Ng YS. Erythropoietin promotes survival of retinal ganglion cells in DBA/2J glaucoma mice. Invest Ophthalmol Vis Sci 2007; 48:1212-8. [PMID: 17325165].
19. Grimm C, Wenzel A, Groszer M, Mayser H, Seeliger M, Samardzija M, Bauer C, Gassmann M, Reme CE. HIF-1-induced erythropoietin in the hypoxic retina protects against light-induced retinal degeneration. Nat Med 2002; 8:718-24. [PMID: 12068288].
20. Wu H, Liu X, Jaenisch R, Lodish HF. Generation of committed erythroid BFU-E and CFU-E progenitors does not require erythropoietin or the erythropoietin receptor. Cell 1995; 83:59-67. [PMID: 7553874].
21. Lin CS, Lim SK, D'Agati V, Costantini F. Differential effects of an erythropoietin receptor gene disruption on primitive and definitive erythropoiesis. Genes Dev 1996; 10:154-64. [PMID: 8566749].
22. Yu X, Shacka JJ, Eells JB, Suarez-Quian C, Przygodzki RM, Beleslin-Cokic B, Lin CS, Nikodem VM, Hempstead

B, Flanders KC, Costantini F, Noguchi CT. Erythropoietin receptor signalling is required for normal brain development. Development 2002; 129:505-16. [PMID: 11807041].

23. Tsai PT, Ohab JJ, Kertesz N, Groszer M, Matter C, Gao J, Liu X, Wu H, Carmichael ST. A critical role of erythropoietin receptor in neurogenesis and post-stroke recovery. J Neurosci 2006; 26:1269-74. [PMID: 16436614].

24. Chan-Ling T, Gock B, Stone J. The effect of oxygen on vasoformative cell division. Evidence that 'physiological hypoxia' is the stimulus for normal retinal vasculogenesis. Invest Ophthalmol Vis Sci 1995; 36:1201-14. [PMID: 7775098].

25. Noguchi CT, Wang L, Rogers HM, Teng R, Jia Y. Survival and proliferative roles of erythropoietin beyond the erythroid lineage. Expert Rev Mol Med 2008; 10:e36-[PMID: 19040789].

26. Kertesz N, Wu J, Chen TH, Sucov HM, Wu H. The role of erythropoietin in regulating angiogenesis. Dev Biol 2004; 276:101-10. [PMID: 15531367].

27. Chung H, Lee H, Lamoke F, Hrushesky WJ, Wood PA, Jahng WJ. Neuroprotective role of erythropoietin by antiapoptosis in the retina. J Neurosci Res 2009; 87:2365-74. [PMID: 19301424].

28. Ashery-Padan R, Marquardt T, Zhou X, Gruss P. Pax6 activity in the lens primordium is required for lens formation and for correct placement of a single retina in the eye. Genes Dev 2000; 14:2701-11. [PMID: 11069887].

29. Le YZ, Zheng L, Zheng W, Ash JD, Agbaga MP, Zhu M, Anderson RE. Mouse opsin promoter-directed Cre recombinase expression in transgenic mice. Mol Vis 2006; 12:389-98. [PMID: 16636658].

30. Madisen L, Zwingman TA, Sunkin SM, Oh SW, Zariwala HA, Gu H, Ng LL, Palmiter RD, Hawrylycz MJ, Jones AR, Lein ES, Zeng H. A robust and high-throughput Cre reporting and characterization system for the whole mouse brain. Nat Neurosci 2010; 13:133-40. [PMID: 20023653].

31. Lange C, Heynen SR, Tanimoto N, Thiersch M, Le YZ, Meneau I, Seeliger MW, Samardzija M, Caprara C, Grimm C. Normoxic activation of hypoxia inducible factors in photoreceptors provides transient protection against light induced retinal degeneration. Invest Ophthalmol Vis Sci 2011; 52:5872-80. [PMID: 21447692].

32. Heynen SR, Meneau I, Caprara C, Samardzija M, Imsand C, Levine EM, Grimm C. CDC42 Is Required for Tissue Lamination and Cell Survival in the Mouse Retina. PLoS ONE 2013; 8:e53806-[PMID: 23372671].

33. Tanimoto N, Muehlfriedel RL, Fischer MD, Fahl E, Humphries P, Biel M, Seeliger MW. Vision tests in the mouse: Functional phenotyping with electroretinography. Front Biosci 2009; 14:2730-7. [PMID: 19273231].

34. Nagao M, Masuda S, Abe S, Ueda M, Sasaki R. Production and ligand-binding characteristics of the soluble form of murine erythropoietin receptor. Biochem Biophys Res Commun 1992; 188:888-97. [PMID: 1445329].

35. Harris KW, Winkelmann JC. Enzyme-linked immunosorbent assay detects a potential soluble form of the erythropoietin receptor in human plasma. Am J Hematol 1996; 52:8-13. [PMID: 8638628].

36. Westphal G, Braun K, Debus J. Detection and quantification of the soluble form of the human erythropoietin receptor (sEpoR) in the growth medium of tumor cell lines and in the plasma of blood samples. Clin Exp Med 2002; 2:45-52. [PMID: 12049189].

37. Jubinsky PT, Krijanovski OI, Nathan DG, Tavernier J, Sieff CA. The beta chain of the interleukin-3 receptor functionally associates with the erythropoietin receptor. Blood 1997; 90:1867-73. [PMID: 9292519].

38. Blake TJ, Jenkins BJ, D'Andrea RJ, Gonda TJ. Functional cross-talk between cytokine receptors revealed by activating mutations in the extracellular domain of the beta-subunit of the GM-CSF receptor. J Leukoc Biol 2002; 72:1246-55. [PMID: 12488507].

39. Luche H, Weber O, Nageswara Rao T, Blum C, Fehling HJ. Faithful activation of an extra-bright red fluorescent protein in "knock-in" Cre-reporter mice ideally suited for lineage tracing studies. Eur J Immunol 2007; 37:43-53. [PMID: 17171761].

40. Caprara C, Thiersch M, Lange C, Joly S, Samardzija M, Grimm C. HIF1A is essential for the development of the intermediate plexus of the retinal vasculature. Invest Ophthalmol Vis Sci 2011; 52:2109-17. [PMID: 21212189].

41. Marquardt T, Ashery-Padan R, Andrejewski N, Scardigli R, Guillemot F, Gruss P. Pax6 is required for the multipotent state of retinal progenitor cells. Cell 2001; 105:43-55. [PMID: 11301001].

42. Elliott S, Busse L, Bass MB, Lu H, Sarosi I, Sinclair AM, Spahr C, Um M, Van G, Begley CG. Anti-Epo receptor antibodies do not predict Epo receptor expression. Blood 2006; 107:1892-5. [PMID: 16249375].

43. Kirkeby A, van Beek J, Nielsen J, Leist M, Helboe L. Functional and immunochemical characterisation of different antibodies against the erythropoietin receptor. J Neurosci Methods 2007; 164:50-8. [PMID: 17524492].

44. Digicaylioglu M, Bichet S, Marti HH, Wenger RH, Rivas LA, Bauer C, Gassmann M. Localization of specific erythropoietin binding sites in defined areas of the mouse brain. Proc Natl Acad Sci USA 1995; 92:3717-20. [PMID: 7731971].

45. Lewczuk P, Hasselblatt M, Kamrowski-Kruck H, Heyer A, Unzicker C, Siren AL, Ehrenreich H. Survival of hippocampal neurons in culture upon hypoxia: effect of erythropoietin. Neuroreport 2000; 11:3485-8. [PMID: 11095504].

46. Ruscher K, Freyer D, Karsch M, Isaev N, Megow D, Sawitzki B, Priller J, Dirnagl U, Meisel A. Erythropoietin is a paracrine mediator of ischemic tolerance in the brain: evidence from an in vitro model. J Neurosci 2002; 22:10291-301. [PMID: 12451129].

47. Sun Y, Zhou C, Polk P, Nanda A, Zhang JH. Mechanisms of erythropoietin-induced brain protection in neonatal

hypoxia-ischemia rat model. J Cereb Blood Flow Metab 2004; 24:259-70. [PMID: 14747752].

48. Chateauvieux S, Grigorakaki C, Morceau F, Dicato M, Diederich M. Erythropoietin, erythropoiesis and beyond. Biochem Pharmacol 2011; 82:1291-303. [PMID: 21782802].

49. Wen TC, Sadamoto Y, Tanaka J, Zhu PX, Nakata K, Ma YJ, Hata R, Sakanaka M. Erythropoietin protects neurons against chemical hypoxia and cerebral ischemic injury by up-regulating Bcl-xL expression. J Neurosci Res 2002; 67:795-803. [PMID: 11891794].

50. Renzi MJ, Farrell FX, Bittner A, Galindo JE, Morton M, Trinh H, Jolliffe LK. Erythropoietin induces changes in gene expression in PC-12 cells. Brain Res Mol Brain Res 2002; 104:86-95. [PMID: 12117554].

51. Chong ZZ, Kang JQ, Maiese K. Apaf-1, Bcl-xL, cytochrome c, and caspase-9 form the critical elements for cerebral vascular protection by erythropoietin. J Cereb Blood Flow Metab 2003; 23:320-30. [PMID: 12621307].

52. Shang YC, Chong ZZ, Wang S, Maiese K. Erythropoietin and Wnt1 govern pathways of mTOR, Apaf-1, and XIAP in inflammatory microglia. Curr Neurovasc Res 2011; 8:270-85. [PMID: 22023617].

53. Hu LM, Luo Y, Zhang J, Lei X, Shen J, Wu Y, Qin M, Unver YB, Zhong Y, Xu GT, Li W. EPO reduces reactive gliosis and stimulates neurotrophin expression in Muller cells. Front Biosci 2011; 3:1541-55. Elite Ed[PMID: 21622158].

54. Bringmann A, Wiedemann P. Müller glial cells in retinal disease. Ophthalmologica 2012; 227:1-19. [PMID: 21921569].

55. Youssoufian HA, Zon LI, Orkin SH, D'andrea AD, Lodish HF. Structure and transcription of the mouse erythropoietin receptor gene. Mol Cell Biol 1990; 10:3675-82. [PMID: 2162479].

56. Hardee ME, Cao Y, Fu P, Jiang X, Zhao Y, Rabbani ZN, Vujaskovic Z, Dewhirst MW, Arcasoy MO. Erythropoietin blockade inhibits the induction of tumor angiogenesis and progression. PLoS ONE 2007; 2:e549-[PMID: 17579721].

57. Colella P, Iodice C, Di Vicino U, Annunziata I, Surace EM, Auricchio A. Non-erythropoietic erythropoietin derivatives protect from light-induced and genetic photoreceptor degeneration. Hum Mol Genet 2011; 20:2251-62. [PMID: 21421996].

58. Chen ZY, Asavaritikrai P, Prchal JT, Noguchi CT. Endogenous erythropoietin signaling is required for normal neural progenitor cell proliferation. J Biol Chem 2007; 282:25875-83. [PMID: 17604282].

59. ed. Cell-intrinsic regulators of proliferation in vertebrate retinal progenitors. Seminars in cell & developmental biology 15(1); 2004; Elsevier; 2004.

60. Soliz J, Gassmann M, Joseph V. Soluble erythropoietin receptor is present in the mouse brain and is required for the ventilatory acclimatization to hypoxia. J Physiol 2007; 583:329-36. [PMID: 17584830].

61. Khankin EV, Mutter WP, Tamez H, Yuan H-T, Karumanchi SA, Thadhani R. Soluble erythropoietin receptor contributes to erythropoietin resistance in end-stage renal disease. PLoS ONE 2010; 5:e9246-[PMID: 20169072].

62. Maynard SE, Min J-Y, Merchan J, Lim K-H, Li J, Mondal S, Libermann TA, Morgan JP, Sellke FW, Stillman IE. Excess placental soluble fms-like tyrosine kinase 1 (sFlt1) may contribute to endothelial dysfunction, hypertension, and proteinuria in preeclampsia. J Clin Invest 2003; 111:649-58. [PMID: 12618519].

63. Venkatesha S, Toporsian M, Lam C, Hanai J. -, Mammoto T, Kim YM, Bdolah Y, Lim K-H, Yuan H-T, Libermann TA. Soluble endoglin contributes to the pathogenesis of preeclampsia. Nat Med 2006; 12:642-9. [PMID: 16751767].

64. Chen F, Xie Z, Wu X, Du W, Wang J, Zhu J, Ji H, Wang Y. Intravitreal Injection of Soluble Erythropoietin Receptor Exacerbates Photoreceptor Cell Apoptosis in a Rat Model of Retinal Detachment. Curr Eye Res 2012; 37:1156-64. [PMID: 22906152].

65. Brugniaux JV, Pialoux V, Foster GE, Duggan CTC, Eliasziw M, Hanly PJ, Poulin MJ. Effects of intermittent hypoxia on erythropoietin, soluble erythropoietin receptor and ventilation in humans. Eur Respir J 2011; 37:880-7. [PMID: 20947680].

66. Ribatti D, Presta M, Vacca A, Ria R, Giuliani R, Dell'Era P, Nico B, Roncali L, Dammacco F. Human erythropoietin induces a pro-angiogenic phenotype in cultured endothelial cells and stimulates neovascularization in vivo. Blood 1999; 93:2627-36. [PMID: 10194442].

67. Anagnostou A, Lee ES, Kessimian N, Levinson R, Steiner M. Erythropoietin has a mitogenic and positive chemotactic effect on endothelial cells. Proc Natl Acad Sci USA 1990; 87:5978-82. [PMID: 2165612].

68. Nakamura-Ishizu A, Kurihara T, Okuno Y, Ozawa Y, Kishi K, Goda N, Tsubota K, Okano H, Suda T, Kubota Y. The formation of an angiogenic astrocyte template is regulated by the neuroretina in a HIF-1-dependent manner. Dev Biol 2012; 363:106-14. [PMID: 22226979].

69. Barron C, Migliaccio AR, Migliaccio G, Jiang Y, Adamson JW, Ottolenghi S. Alternatively spliced mRNAs encoding soluble isoforms of the erythropoietin receptor in murine cell lines and bone marrow. Gene 1994; 147:263-8. [PMID: 7926812].

Articles are provided courtesy of Emory University and the Zhongshan Ophthalmic Center, Sun Yat-sen University, P.R. China. The print version of this article was created on 14 March 2014. This reflects all typographical corrections and errata to the article through that date. Details of any changes may be found in the online version of the article.